Chemistry and DNA Alkylation Reactions of Aziridinyl Quinones: Development of an Efficient Alkylating Agent of the Phosphate Backbone†

Edward B. Skibo* and Chengguo Xing

Department of Chemistry and Biochemistry, Box 871604, Arizona State University, Tempe, Arizona 85287-1604

Received May 21, 1998; Revised Manuscript Received September 2, 1998

ABSTRACT: Described herein are detailed hydrolytic studies of a series of aziridinyl quinones, which trap nucleophiles when protonated. This study provided a compilation of the rate constants for nucleophile trapping and of the pK_a values for the protonated aziridinyl quinones. A linear free energy relationship, including the antitumor agent DZQ, as well as other synthetic quinone derivatives, was obtained as a result of this study. Protonated DZQ has the relatively high pK_a value of 3.8, which explains the enhanced cross-linking of DNA by DZQ and other related aziridinyl quinones at pH 4. The literature often shows aziridinyl quinone protonation occurring at the aziridinyl nitrogen, but the dependence of pK_a values on quinone substituents indicates the presence of delocalization, which must arise from *O*-protonation. Also investigated were the DNA alkylation reactions of protonated aziridinyl quinones. At the outset of this study, we postulated that these "hard" electrophiles would alkylate the phosphate backbone of DNA. Bulk DNA is up to 35% alkylated by protonated aziridinyl quinones as judged by the incorporation of the quinone chromophore into the DNA. The presence of phosphate alkylation was verified by a ^{1}H−^{31}P NMR correlation experiment with DZQ-alkylated hexamer. Our modeling studies present a new picture of DZQ alkylation of DNA, where there is competition between N(7) and phosphate alkylation. The conclusions of this part of our study are that the phosphate backbone should be considered as a possible target of any DNA-alkylating agent and that an assessment of phosphate alkylation is best made with a ^{1}H−^{31}P NMR correlation experiment. Finally, the benzimidazole-based aziridinyl quinone **2** was observed to undergo aziridine ring opening followed by hydrolytic removal of the aminoethyl group from the quinone ring. This reaction was used to tag the phosphate backbone of DNA with aminoethyl groups. Such tags render anionic phosphates cationic and could also be employed as points of attachment for chromophores, spin labels, or other moieties to DNA.

The guanine N(7) position of DNA is the usual site of alkylation by the aziridinyl quinones and hydroquinones. Theoretical studies have shown that the guanine N(7) position is the most reactive nucleophile of DNA (*1*−*4*). For example, the benzoquinone analogues DZQ and AZQ, shown in Chart 1, are known to cross-link DNA by alkylation of guanine N(7) residues upon reduction to the hydroquinone (*5*−*10*). In contrast, the PBI reductive alkylating agents developed in this laboratory target the oxygen anion of the phosphate backbone (*11, 12*).

Our explanation for the choice of the phosphate anion by the PBI reductive alkylating agent was based on the electron-deficient nature of the benzimidazole ring system of the PBI (*12*). The electron-deficient character supposedly results in partial carbocation formation in the aziridine ring resulting in the alkylation of the "hard" nucleophile represented by the phosphate backbone.

Alkyation of the phosphate backbone by a variety of agents is actually well-known (*13*−*16*). The presence of carbocation or partial carbocation character in the alkylating agent was thought to be a reason for the preferred reaction at the phosphate backbone (*13*). The importance of electronic character in the selection of the DNA alkylation site is illustrated by epoxides: normally epoxides alkylate DNA at the guanine N(7) position (*17*) as well as the O(6) and N(2) positions (*18*), but electron-deficient analogues alkylate the phosphate backbone (*19*). Considering these precedents,

Chart 1

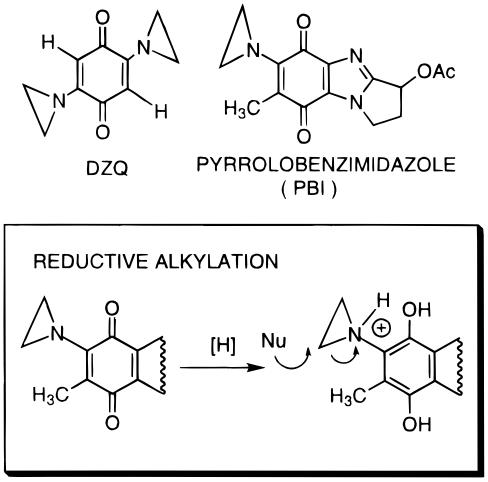

† This work was supported by the National Science Foundation and the Arizona Disease Control Commission.

* To whom correspondence should be addressed. Telephone: 602-965-3581. Fax: 602-965-2747. E-mail: ESkibo@ASU.edu.

10.1021/bi981204j CCC: $15.00
Published on Web 10/07/1998

Chart 2

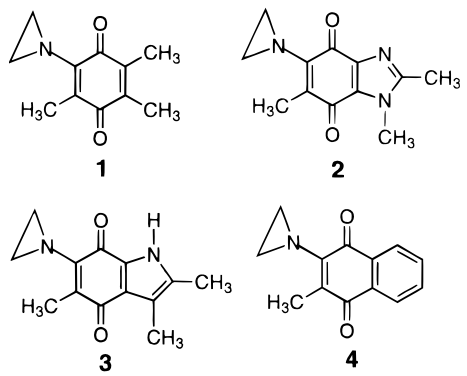

Scheme 1

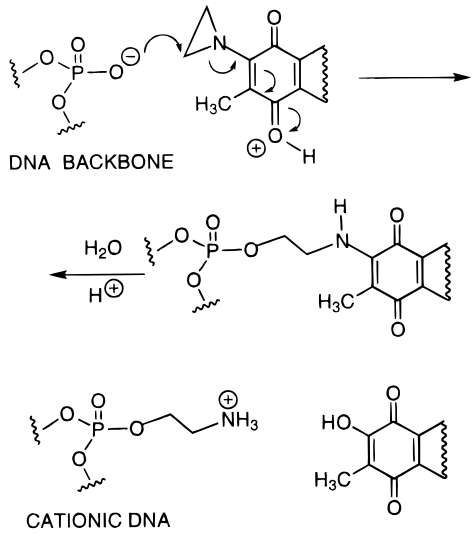

the aziridinyl quinones themselves, without reduction to the hydroquinones, should be effective alkylating agents of the phosphate backbone.

To investigate this possibility, the oxidized forms of **1**−**4** in Chart 2, along with DZQ, were studied in aqueous buffer with respect to their hydrolytic chemistry and nucleophile selectivity in reactions with DNA and 5′-deoxyguanosine monophosphate (5′-dGMP).

The pK_a values of DZQ and other aziridinyl quinones were determined from pH−rate profiles, and a free energy plot was obtained for the nucleophile trapping of aziridinyl quinones. With these results in hand, we were able to develop an efficient alkylating agent for the phosphate backbone. As illustrated in Scheme 1, our hydrolytic studies permitted the removal of the quinone moiety under mild conditions resulting in the formation of a cationic aminoethyl ester of the phosphate backbone. Such altered backbones of DNA are of interest in the context of antisense/antigene development (*20*−*23*). Indeed, the preparation of cationic backbone derivatives (*24*, *25*) and other derivatives (*26*) of DNA is currently of great interest. While altered backbones of DNA, cationic and otherwise, usually involve extensive synthesis, the altered DNAs described herein can be prepared from native DNA in one step by incubation with an aziridinyl quinone.

MATERIALS AND METHODS

All analytically pure compounds were dried under high vacuum in a drying pistol heated with refluxing methanol. Fremy salt was purchased from Aldrich, stored over calcium chloride desiccant in a refrigerator, and used within 1 month. Some compounds contained fractional amounts of water of crystallization that was determined from the elemental analyses found. Elemental analyses were run at Atlantic Microlab, Inc., Norcross, GA. Uncorrected melting points and decomposition points were determined with a Mel-Temp apparatus. All TLC were run with silica gel plates with fluorescent indicator, employing a variety of solvents. IR spectra were taken as KBr pellets or thin films; the strongest IR absorbances are reported. ^{1}H and ^{13}C NMR spectra were obtained on a 300-MHz spectrometer, and chemical shifts are reported relative to TMS. ^{31}P NMR spectra are referenced to phosphoric acid, and ^{1}H-detected ^{1}H−^{31}P correlation spectra were run with $J = 20$ Hz. UV−visible spectroscopic/kinetic studies were carried out on a OLIS modified Cary 14 spectrometer. Computer fits of rate laws were carried out with a Scientist mathematical fitting program. Poly(dG-C)·poly(dG-C) and poly(dA-T)·poly(dA-T) were purchased from Sigma, and d(CGATCG)$_2$ and CG were prepared with a DNA synthesizer.

2,3,5-Trimethyl-1,4-benzoquinone. To a stirred solution of 500 mg (3.29 mmol) of 2,3,5-trimethyl-1,4-hydroquinone in 37 mL of H_2O and 3 mL of concentrated H_2SO_4, held at room temperature, was added a solution of 3.8 g of $K_2Cr_2O_7$ in 23 mL of H_2O and 2 mL of concentrated H_2SO_4. After stirring for 2.5 h, the solution was extracted four times with 50-mL portions of chloroform. The extracts were dried over Na_2SO_4 and then concentrated to a residue, which was purified by flash chromatography on silica gel using chloroform as the eluent. The isolated product was recrystallized from diethyl ether: 348 mg (72%) yield; ^{1}H NMR ($CDCl_3$) δ 6.557 (1H, q, $J = 2$ Hz, quinone ring proton), 2.039 (3H, d, $J = 2$ Hz, 5-methyl), 2.033 and 2.011 (6H, 2q, $J = 1$ Hz, methyls).

*2-Aziridinyl-3,5,6-trimethyl-1,4-benzoquinone (**1**).* To a mixture of 200 mg (1.33 mmol) of 2,3,5-trimethyl-1,4-benzoquinone in 30 mL of methanol was added 3 mL of ethylenimine. The solution was stirred at room temperature for 22 h and then concentrated to a residue, which was purified by a flash chromatography using 99% $CHCl_3$/1% MeOH as the eluent. The isolated product was recrystallized from diethyl ether: 129 mg (50%) yield; mp 87−88 °C; TLC (chloroform/methanol, 95:5) $R_f = 0.70$; IR (KBr pellet) 2999, 2924, 2854, 2362, 1647, 1606, 1580, 1377, 1292, 1167 cm^{-1}; ^{1}HNMR ($CDCl_3$) δ 2.24 (4H, s, ethylenimine proton), 2.0 (3H, s, 3-methyl group), 2.00 and 1.98 (6H, 2q, $J = 1$ Hz, methyl groups); MS (EI mode) *m/z* 191 (M^+) 176 ($M^+ - CH_3$) 162, 148, 135, 120, 107, 91, 81. Anal. Calcd for $C_{11}H_{13}NO_2$: C, 69.09; H, 6.85; N, 7.32. Found: C, 68.86; H, 6.92; N, 7.26.

*2-Aziridinyl-3-methyl-1,4-naphthoquinone (**4**).* To 340 mg (1.98 mmol) of 2-methyl-1,4-naphthoquinone in 10 mL of methanol was added 3 mL of ethylenimine, and the reaction was stirred at room temperature for 5 h. The solution was vacuum-dried to afford a yellow syrup, which was purified by flash chromatography on silica gel using $CHCl_3$ as eluent. The product was then dried and recrystallized with chloroform/hexane: 215 mg (51%) yield; mp 117−119 °C; TLC ($CHCl_3$) $R_f = 0.13$; ^{1}H NMR ($CDCl_3$) δ 8.0 (2H, m, 5,8-protons), 7.650 (2H, m, 6,7-protons), 2.37 (4H, s, ethylenimine protons), 2.20 (3H, s, methyl); IR (KBr pellet) 2932,

2364, 2346, 1664, 1637, 1597, 1572, 1381, 1334, 1282, 1168, 949, 723 cm^{-1}; MS (EI mode) *m/z* 213 (M^+), 198 ($M^+ - CH_3$), 184, 168, 156, 129, 115. Anal. Calcd for $C_{13}H_{11}NO_2$: C, 73.22; H, 5.20; N, 6.57. Found: C, 73.08; H, 5.18; N, 6.51.

*2,3,5-Trimethylindole-4,7-dione (**6**)* was prepared from 2,3,5-trimethylindole (**5**) by the following two-step synthesis.

To a solution of 500 mg (3.14 mmol) of 2,3,5-trimethylindole with 15 mg of PtO_2 in 20 mL of ethanol was added a solution of 17 mL of 48% aqueous HBF_4. This solution was reduced by H_2 at 10 psi for 1 h, at which time the color faded. The catalyst was removed by filtration through Celite, and the filtrate was extracted five times with 50-mL portions of chloroform. The extracts were washed with saturated sodium bicarbonate, and the aqueous phase was extracted two times with 50-mL portions of chloroform. The combined chloroform extracts were dried over Na_2SO_4 and then concentrated to an oil, which was purified by silica gel chromatography using $CHCl_3$ as the eluent. The isolated 2,3,5-trimethylindoline fractions were concentrated to a colorless liquid which turned brown with time: 312 mg (62%) yield; TLC (chloroform/hexane, 90:10) $R_f = 0.5$; ^1H NMR ($CDCl_3$) δ 6.90 (1H, s, Ar), 6.82 (1H, d, $J = 8$ Hz, Ar), 6.55 (1H, d, $J = 8$ Hz, Ar), 3.91 (1H, m, 2-indoline protons), 3.62 (1H, bs, N−H), 3.211 (1H, m, 3-indoline protons), 2.276 (3H, s, 5-methyl), 1.315 and 1.167 (6H, 2d, $J = 6$ Hz, 2,3-dimethyls); MS (El mode) *m/z* 161 (M^+), 146 ($M^+ - CH_3$), 131, 115, 103.

To a solution of 312 mg (1.94 mmol) of 2,3,5-trimethylindoline in 20 mL of H_2O containing 172 mg of potassium phosphate monobasic was added a solution of 1.0 g Fremy's salt in 150 mL of H_2O containing 500 mg of potassium phosphate monobasic. The solution was stirred at room temperature for 1.5 h and then extracted four times with 50-mL portions of chloroform. The combined extract was dried over Na_2SO_4 and evaporated to a residue, which was purified by flash chromatography on silica gel using chloroform as the eluent. Concentration of the product fractions provided **6** as a dark-red solid: 104 mg (28.7%) yield; mp 185−187 °C dec; TLC ($CHCl_3$/MeOH, 95:5) $R_f = 0.66$; IR (KBr pellet) 3209, 3049, 2928, 2854, 2361, 2343, 1633, 1597, 1482, 1103, 810 cm^{-1}; ^1H NMR ($CDCl_3$) δ 9.300 (1H, bs, N−H), 6.394 (1H, q, $J = 2$ Hz, proton on quinone ring), 2.25 and 2.245 (6H, 2s, 2,3-dimethyl), 2.06 (3H, d, $J = 2$ Hz, 5-methyl); MS (El mode) *m/z* 189 (M^+), 174 ($M^+ - CH_3$), 161 ($M^+ - CO$), 149, 132, 121. Anal. Calcd for $C_{11}H_{11}NO_2$: C, 69.82; H, 5.86; N, 7.40. Found: C, 69.96; H, 5.84; N, 7.33.

*6-Aziridinyl-2,3,5-trimethylindole-4,7-dione (**3**).* To a solution of 23.5 mg (0.12 mmol) of **6** in 2.5 mL of methanol was added 1 mL of ethylenimine, and the resulting solution was stirred at room temperature for 7 days. The solution was then evaporated to dryness, and the resulting residue was purified by flash chromatography using 1% methanol in chloroform as the eluent. The product was recrystallized from chloroform/hexane to afford a red solid: 19.6 mg (70%) yield; mp 250 °C dec; TLC (chloroform/methanol, 95:5) $R_f = 0.55$; IR (KBr pellet) 3238, 2922, 2361, 2343, 1637, 1591, 1097, 798 cm^{-1}; ^1H NMR ($CDCl_3$) δ 9.124 (1H, bs, N−H), 2.270 (4H, s, aziridinyl), 2.252, 2.225, and 2.056 (9H, 3s, methyls); MS (El mode) *m/z* 230 (M^+), 215 ($M^+ - CH_3$), 201, 189, 174, 160. Anal. Calcd for $C_{13}H_{14}N_2O_2$: C, 67.81; H, 6.13; N, 12.17. Found: C, 67.63; H, 6.03; N, 12.05.

Kinetic Studies of Nucleophile-Mediated Ring Opening of Aziridinyl Quinones. A dimethyl sulfoxide solution of the aziridinyl quinone under study was added to an aqueous buffer held at 30 °C containing 0.15 M buffer species (chloroacetate, formate, acetate, phosphate) and varying concentrations of potassium chloride. The amount of dimethyl sulfoxide was always constant and small enough so as not to produce a solvent effect; 50 μL in a 3000-μL final reaction concentration. The buffer species, if present in high enough concentration, will be part of the rate law for hydrolysis. For example, only high concentrations of acetate (~1 M) result in trapping of acetate by the aziridinyl quinone. To minimize the presence of buffer species in the rate law, relatively large amounts of potassium chloride were added to the reactions and the buffer concentration was held constant. The course of reactions was followed spectrophotometrically at the λ_{max} of the aziridinyl quinone; ring opening of **1** was followed at 288 nm, and that of DZQ was followed at 342 nm. The ring opening of the other aziridinyl quinones also was followed in this wavelength region. When a pK_a was reached, the λ_{max} of the aziridinyl quinone shifted and a repetitive scan experiment was carried out to determine the best wavelength to follow the reaction. Absorbance versus time plots were computer-fit to a first-order or a two consecutive first-order rate law. DZQ hydrolysis followed a two consecutive first-order rate law due to the successive opening of two aziridine rings, while **1** and **4** hydrolyzed by a single first-order rate law. The hydrolysis of compounds **2** and **3** followed a two consecutive first-order rate law due to nucleophile trapping followed by rapid hydrolysis of the ring-opened product. First-order rate constants were plotted as a function of chloride concentration to afford the second-order rate constant for chloride trapping as the slope and the pseudo-first-order rate constant for water trapping as the intercept. The concentration of water is essentially constant, and its activity is considered to be 1. The pseudo-first-order water-trapping term could also include the rate constant for trapping of the aziridinyl quinone by buffer species employed to hold pH. However, at the buffer concentration employed (0.15 M) no buffer-trapping products (trapping by acetate, formate, chloroacetate) were observed.

Product Studies

Chloride- and Water-Mediated Ring Opening of Aziridinyl Quinones. The aziridinyl quinone (~1 mmol) was dissolved in 500 λ of dimethyl sulfoxide and added to 25 mL of 0.05 M pH 3.9 acetate buffer containing 0.95 M KCl. Alternatively, lower pH buffers were used, such as 0.05 M pH 2.9 formate or 0.05 M pH 3.3 formate buffer, both containing 0.95 M KCl. These lower pH buffers provided the same products over a shorter reaction time. The relatively insoluble indole **3** was hydrolyzed in a 250-mL volume of buffer. The reactions were stirred at 30 °C over a period of time determined from the kinetic study, usually 2−5 h. The product was removed by extraction with chloroform, and the extracts were dried over sodium sulfate. The extracts were concentrated to dryness, and the residue was recrystallized from chloroform/hexane. The chloride-trapping products thus obtained were spectrally pure. An efficient way of preparing the chloride-trapping products was to dissolve the benzoquinone in DMSO and then add concentrated hydrochloric acid. Addition of ice immediately thereafter afforded crystal-

lized chloride-trapping product. Preparation of water-trapping products was also carried out in buffers as described above except that KCl was not present.

Provided below are the physical properties (or references to previous reports) of chloride-trapping products (designated with **A**) and water-trapping products (designated with **B**). The water-trapping products were characterized only for benzoquinones **1** and DZQ.

*2-(2-Chloroethylamino)-3,5,6-trimethyl-1,4-benzoquinone (**1A**)*: mp 71−73 °C; TLC ($CHCl_3$/hexane, 50:50) R_f = 0.45; IR (KBr pellet) 3337, 1662, 1585, 1510, 1276, 1253 cm^{-1}; ^1H NMR ($CDCl_3$) δ 5.59 (1H, bs, amino proton), 3.76 (2H, t, J = 6 Hz, methylene), 3.63 (2H, doublet of triplets, J = 1.2 Hz and J = 6 Hz, methylene), 2.03 (3H, s, methyl) 2.02 (3H, q, J = 1.2 Hz, methyl), 1.98 (3H, q, J = 1.2 Hz, methyl); MS (EI mode) m/z 227 and 229 (M^+ ^{35}Cl, ^{37}Cl), 191 (M^+ − HCl), 178, 163.

*2-(2-Hydroxyethylamino)-3,5,6-trimethyl-1,4-benzoquinone (**1B**)*: mp 82−85 °C dec; TLC ($CHCl_3$/MeOH, 85:15) R_f = 0.48; IR (KBr pellet) 3464, 2924, 2854, 2361, 1638, 1516, 1057, 723 cm^{-1}; ^1H NMR ($CDCl_3$) δ 3.800 (2H, t, J = 5.7 Hz, methylene), 3.605 (2H, t, J = 5.7 Hz, methylene) 2.056 (3H, s, methyl), 2.027 (3H, q, J = 1.2 Hz, methyl), 1.970 (3H, q, J = 1.2 Hz, methyl); MS (EI mode) m/z 209 (M^+), 191 ($M^+ - H_2O$), 178, 163. Anal. Calcd for $C_{11}H_{15}NO_3$: C, 63.13; H, 7.23; N, 6.69. Found: C, 63.07; H, 7.22; N, 6.62.

*5-(2-Chloroethylamino)-1,2,6-trimethylbenzimidazole-4,7-dione (**2A**)*: mp 103−105 °C dec; TLC ($CHCl_3$/MeOH, 90:10) R_f = 0.57; IR (KBr pellet) 3242, 2978, 2874, 1676, 1616, 1593, 1518, 1471, 1437, 1292, 1130, 1049, 989, 742 cm^{-1}; ^1H NMR ($CDCl_3$) δ 5.84 (1H, bs, amino proton), 3.88 (1H, s, 1-methyl), 3.86 (2H, m, methylene), 3.65 (2H, t, J = 6 Hz, methylene), 2.46 and 2.05(6H, 2s, 2,6-dimethyl); MS (EI mode) m/z 267 and 269 (M^+ ^{35}Cl, ^{37}Cl), 232 (M^+ − Cl), 218 ($M^+ - CH_2Cl$), 204, 191, 123.

*6-(2-Chloroethylamino)-2,3,5-trimethylindole-4,7-dione (**3A**)*: mp 190−192 °C; TLC ($CHCl_3$/MeOH, 95:5) R_f = 0.50; IR (KBr pellet) 3447, 3240, 2926, 2362, 1655, 1618, 1508, 1284, 1148, 754 cm^{-1}; ^1H NMR ($CDCl_3$) δ 9.61 (1H, bs, indole proton), 5.61 (1H, bs, amino NH), 3.79 (2H, q, J = 6 Hz, methylene), 3.65 (2H, t, J = 6.0 Hz methylene), 2.26, 2.24, and 2.03 (9H, 3s, methyls); MS (EI mode) m/z 266 and 268 (M^+ with ^{35}Cl, ^{37}Cl), 230 (M^+−HCl), 215, 189. Anal. Calcd for $C_{13}H_{15}ClN_2O_2$: C, 58.54; H, 5.67; N, 10.50. Found: C, 58.45; H, 5.53; N, 10.16.

*2-(2-Chloroethylamino)-3-methylnaphthalene-1,4-dione (**4A**)*: mp 134−136 °C; TLC ($CHCl_3$/MeOH, 95:5) R_f = 0.66; IR (KBr pellet) 3311, 1676, 1602, 1570, 1518, 1467, 1458, 1344, 1315, 1302, 1276, 1255, 729 cm^{-1}; ^1H NMR ($CDCl_3$) δ 8.11−7.56 (4H, m, aromatic protons), 5.84 (1H, bs, amino proton), 3.89 (2H, q, J = 6 Hz, methylene), 3.69 (2H, t, J = 6 Hz, methylene), 2.20 (3H, s, methyl); MS (EI mode) m/z 249 and 251 (M^+ ^{35}Cl, ^{37}Cl), 213 (M^+ − HCl), 200. Anal. Calcd for $C_{13}H_{12}ClNO_2$: C, 62.53; H, 4.84; N, 5.61. Found: C, 62.65; H, 4.83; N, 5.66.

Hydrolysis of Ring-Opened Aziridinyl Quinones. A solution of 0.024 mmol of **2** or **3** in 20 mL of dimethyl sulfoxide was added to 250 mL of 0.05 M pH 2.97 acetate buffer containing 0.95 M KCl, and the resulting reaction mixture was stirred for either 30 min (**2**) or 6 h (**3**). For **3**, the reaction volume can be decreased substantially because of its greater solubility in aqueous buffer. The reaction mixture was extracted three times with 20-mL portions of chloroform, and the combined extracts were then washed two times with 15 mL of water and dried over Na_2SO_4. The compound was purified by flash chromatography on silica gel employing methanol/chloroform (2:98) as the eluent.

*6-Hydroxy-2,3,5-trimethylindole-4,7-dione (**7**)*: mp 245 °C dec; TLC (chloroform/methanol, 90:10) R_f = 0.64; IR (KBr pellet) 3358, 3227, 2924, 2856, 2361, 1624, 1483, 1381, 1340, 1257, 1097, 752 cm^{-1}; ^1H NMR (dimethyl sulfoxide-d_6) δ 12.29 (1H, bs, indole NH), 10.0 (1H, s, OH), 2.13 and 2.10 (6H, 2s, 2,3-dimethyl), 1.72 (3H, s, 5-methyl); MS (EI mode) m/z 205 (M^+), 190 ($M^+ - CH_3$), 177 (M^+ − CO), 160, 148, 134, 122. Anal. Calcd for $C_{11}H_{11}NO_3$: C, 64.38; H, 5.40; N, 6.83. Found: C, 65.12; H, 5.58; N, 6.71.

*5-Hydroxy-1,2,6-trimethylbenzimidazole-4,7-dione (**8**)*: mp 222−225 °C; TLC (chloroform/methanol, 90:10) R_f = 0.38; IR (KBr pellet) 3412, 2926, 2376, 2330, 1685, 1643, 1543, 1475, 1244, 973, 783 cm^{-1}; ^1H NMR ($CDCl_3$) δ 7.19 (1H, bs, hydroxy), 3.90, 2.49, and 1.96 (9H, 3s, 1,2,6-trimethyl); MS (EI mode) m/z 206 (M^+), 191 ($M^+ - CH_3$), 178 (M^+ − CO), 163, 149, 121, 109.

Reaction of 5′-dGMP with DZQ in pH 3.96 Buffer. A solution consisting of 41 mg (0.21 mmol) of DZQ in 200 μL of dimethyl sulfoxide was added to a solution consisting of 188 mg (0.42 mmol) of 5′-dGMP disodium salt trihydrate in 2 mL of water and 100 μL of 1 M pH 3.96 acetate buffer. The reaction was incubated for 12 h at 30 °C, and the solids were separated as a pellet by centrifugation at 12000*g*. The pellet was washed with dimethyl sulfoxide and then with water and finally with ethanol to afford pure **9**: 9.3 mg (12%) yield; ^1H NMR (DMSO-d_6) δ 10.77 (1H, bs, purine NH), 7.76 (1H, s, 8-H), 7.71 and 7.42 (2H, 2t, NH coupled to methylene), 6.09 (2H, s, amino), 5.29 and 5.23 (2H, 2s, quinone ring protons), 5.299 (1H, t, J = 6 Hz, hydroxyl), 4.32 (2H, t, J = 6 Hz, methylene of ethylene tether attached to N-7), 3.55 and 3.16 (6H, 2m, other methylenes of ethylene tether); MS (EI mode) m/z 341 ($M^+ - H_2O$).

*Reaction of 5′-dGMP with **1** in pH 3.96 Buffer.* A solution of 35.6 mg (0.19 mmol) of **1** in 2 mL of dimethyl sulfoxide was added to a solution consisting of 188 mg (0.42 mmol) of 5′-dGMP disodium salt trihydrate in 6.5 mL of water and 1.5 mL of 1 M pH 3.96 acetate buffer. The reaction mixture was stirred for 3.5 h at room temperature. Hydrolysis products of **1** were removed by extraction with 30 mL of chloroform, and the aqueous layer was placed on a 100-mL Baker phenyl reverse-phase column prepared with water. Products **10**, **11**, and **12** were eluded from the column with water in trace quantities; the major products were the water and acetate trapping products found in the chloroform. To follow are the physical properties of **10**−**12**.

10: 0.77 mg (0.53%); TLC (*n*-butanol/acetic acid/water, 5:3:2) R_f = 0.18; ^1H NMR (D_2O) δ 7.87 (1H, s, purine CH), 6.01 (1H, t, J = 6.5 Hz, C1′), 4.57 (1H, m, C3′), 4.0 and 3.8 (5H, 2m, methylene of ethylene linkage attached to phosphate, C5′ and C5″, C4′), 3.44 (2H, m, methylene of ethylene linkage attached to nitrogen), 2.56 and 2.30 (2H, 2m, 2′), 1.79, 1.72, and 1.66 (9H, 3s, quinone methyls); ^{31}P NMR (D_2O) δ −1.6 coupled to 3.78 (methylene of ethylene linkage attached to phosphate), 3.95 and 3.97 (C5′ and C5″).

11: 0.48 mg (0.6%); TLC (*n*-butanol/acetic acid/water, 5:3:2) R_f = 0.16; ^1H NMR (D_2O) δ 6.08 (1H, t, J = 0.8 Hz, C1′), 4.29 and 3.90 (2H, m, C3′ and C4′), 3.90 (2H, m, C5′

and C5″), 4.09 (2H, t, $J = 5.4$ Hz, ethylene protons bound to phosphate), 3.84 (2H, m, $J = 5.4$ Hz, ethylene protons bound to nitrogen), 2.60 and 2.42 (2H, m, C2′), 1.79 (3H, s, 3-methyl), 1.68 and 1.65 (6H, q, $J = 2$ Hz, 5,6-dimethyl).

12: 0.83 mg (1.3%); TLC (chloroform/methanol, 9:1) $R_f = 0.12$; ^{1}H NMR (dimethyl sulfoxide-d_6) δ 7.68 (1H, s, purine CH), 6.32 (2H, bs, NH_2), 6.08 (1H, bs, NH), 4.29 (2H, t, $J = 5.2$ Hz, ethylene protons bound to guanine base), 3.82 (2H, m, $J = 5.2$ Hz, ethylene protons bound to nitrogen), 1.85, 1.77, 1.75 (9H, s, quinone methyls); MS (EI mode) *m*/*z* 342 (M^+), 191 (M^+ − trimethylquinone), 178, 167, 152, 138, 97.

*Reaction of 5′-dGMP with **2** in pH 3.96 Buffer.* A solution of 26 mg (0.11 mmol) of **2** in 1 mL of DMSO was added to a solution of 101 mg (0.29 mmol) of 5′-dGMP disodium salt trihydrate in 1.5 mL of 1 M pH 3.96 acetate buffer and 6.0 mL of water. The resulting mixture was stirred at room temperature for 1 day and then extracted three times with 20 mL of chloroform to remove hydrolysis products. The deep-blue aqueous layer was concentrated to dryness to remove all the DMSO. The residue was dissolved in a small volume of water and placed on a 100-mL Baker phenyl reverse-phase column prepared with water. The unreacted 5′-dGMP and the aminoethyl phosphate **14** eluded together as the first fraction followed by the blue band containing **13**. Pure **14** was obtained by incubating the purified **13** in 0.15 M pH 3.96 acetate buffer for 12 h and then removing buffer salts by reverse-phase chromatography.

13: ∼2% yield; TLC (2-propanol/ammonia/water, 7:1:2) $R_f = 0.39$; ^{1}H NMR (D_2O), assignments based on COSY experiment, δ 7.81 (1H, s, purine CH), 5.85 (1H, t, $J = 6$ Hz, C1′), 4.49 (1H, m, C3′), 4.03(1H, m, 4′), 3.98 and 3.87 (2H, 2m, methylene of ethylene linkage attached to phosphate), 3.92 and 3.83 (2H, m, C5′ and C5″), 3.54 (3H, s, 1-methyl), 3.51 (2H, m, methylene of ethylene linkage attached to nitrogen), 2.48 and 2.30 (2H, 2m, C2′), 2.22 (3H, s, 2-methyl), 1.56 (3H, s, 6-methyl); ^{31}P NMR (D_2O) δ 1.447 coupled to 3.98 and 3.87 (methylene of ethylene linkage attached to phosphate), 3.92 and 3.83 (5′ and 5″), and long-range coupled to 4.03 and 3.51 (4′ and methylene of ethylene linkage attached to nitrogen).

14: ∼2% yield; TLC (2-propanol/ammonia/water, 7:1:2) $R_f = 0.35$; ^{1}H NMR (D_2O), assignments based on COSY experiment, δ 7.95 (1H, s, purine CH), 6.21 (1H, t, $J = 6$ Hz, C1′), 4.59 (1H, m, C3′), 4.11 (1H, m, C4′), 3.95 (2H, t, $J = 4$ Hz, C 5′ and C5″), 3.82 (2H, m, methylene of ethylene linkage attached to phosphate), 3.03 (2H, t, $J = 4.4$ Hz, methylene of ethylene linkage attached to nitrogen), 2.72 and 2.44 (2H, 2m, C2′); ^{31}P NMR (D_2O) δ 1.056 coupled to 3.95 (5′ and 5″), 3.82 (methylene of ethylene linkage attached to phosphate), and long-range coupled to 4.11 and 3.03 (4′ and methylene of ethylene linkage attached to nitrogen).

*Reaction of **1**−**4** and DZQ with Poly(dG-C)·Poly(dG-C) and Poly(dA-T)·Poly(dA-T) in pH 3.96 Buffer.* To a solution of the DNA, 25 units (∼1.6 mg), in 1 mL of 0.1 M pH 3.96 acetate buffer was added a 3-fold base pair excess of the quinone dissolved in 300 μL of dimethyl sulfoxide. Reactions were incubated for 12 h at 30 °C, the pH was adjusted with 0.3 M pH 5.1 acetate, and the mixture was diluted with 2 volumes of ethanol. After the solution was chilled at −25 °C for 2 h, a DNA pellet was obtained by centrifugation at 12000*g* for 20 min. The pellet was dissolved in 1 mL of water and reprecipitated as described above. The DNA pellet was then dried, weighed, and dissolved in 1 mL of water. An absorbance measurement at the λ_{max} of the amino quinone was used to calculate the percent alkylation as follows: The extinction coefficient of a ring-opened product (usually the chloroethylamino derivative) of the aziridinyl quinone used in the DNA alkylation was used to calculate the milligrams of adduct in the DNA sample. The adduct weight was subtracted from the total weight of the DNA sample, and the result was divided by the base pair molecular weight of 662 and 661 for G-C and A-T, respectively, to provide the moles of base pairs in the sample. From the moles of base pairs and moles of adduct in the sample, the percent alkylation was determined.

*Reaction of DZQ and **2** with d(CGATCG)$_2$ in pH 3.96 Buffer.* To a solution of 4−6 mg of this DNA in 1 mL of 0.1 M pH 3.96 acetate buffer was added a 10-fold base pair excess of **2** or DZQ dissolved in 300 μL of dimethyl sulfoxide. To combine these solutions completely, a 1-mL chaser of water was added to the reaction mixture. Reactions were incubated for 12 h at 30 °C, the pH was adjusted with 0.3 M in pH 5.1 acetate buffer, and then the mixture was diluted with 2 volumes of ethanol. After the solution was chilled at −25 °C for 2 h, a DNA pellet was obtained by centrifugation at 12000*g* for 20 min. The DNA pellet was dissolved in 1 mL of water and reprecipitated as described above. The DZQ-treated DNA, which weighed 3.9 mg (starting with 4 mg) upon drying, was dissolved in 0.7 mL of 0.1 M pD 7.5 phosphate buffer containing 33 mM KCl. The solids were removed by centrifugation, and the ^{1}H−^{31}P correlation spectrum shown in Figure 8 was obtained. The **2**-treated deep-blue DNA, which weighed 4.5 mg (starting with 6 mg), was dissolved in D_2O and the solution lypophilized to dryness. After repeating the dissolution/lypophilization process two more times, a ^{1}H NMR and ^{1}H−^{31}P correlation spectra were obtained.

Preparation of Aminoethyl Phosphate Esters of the DNA Backbone. The **2**-treated DNA obtained above was heated at 50 °C in 0.15 M pH 3.96 buffer for 2 h. The solution was adjusted to 0.3 M in pH 5.1 acetate buffer and then diluted with 2 volumes of ethanol. After chilling the solution at −25 °C for 12 h, a DNA pellet of **16** was obtained by centrifugation at 12000*g* for 20 min. The altered DNA does not readily precipitate from solution, and a longer than usual chilling time is required.

The attempted alkylation of 3 mg (0.005 mmol) of the GC 2-mer to afford **15** was carried out in 0.15 M pH 3.96 buffer containing 3.25 mg of **2** for 12 h. The completed reaction was placed on a 20-mL Baker phenyl reverse-phase column prepared with water. The unreacted starting material along with a trace amount of **15** was eluted with water.

RESULTS AND DISCUSSION

Synthesis of Aziridinyl Quinones. AZQ (*27*), DZQ (*28*), and **2** (*29*) were synthesized as described in the literature. Compound **1** was prepared by aziridination of 2,3,5-trimethylbenzoquinone, which was prepared by dichromate oxidation of the commercially available hydroquinone derivative. Similarly, **4** was prepared by aziridination of the commercially available naphthoquinone, respectively. The known indole **5** (*30*) was converted to **6** by a convenient

Scheme 2

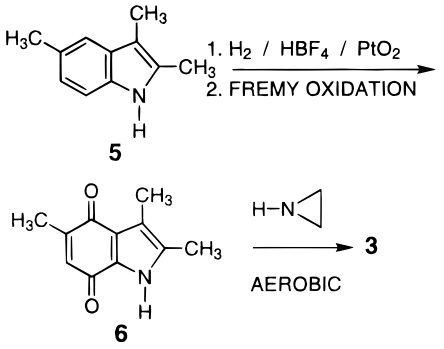

procedure involving reduction of **5** to the indoline followed by Fremy oxidation (Scheme 2). The indoline is an aminobenzene derivative, which is a class of compound known to undergo Fremy oxidations readily (*31*). The Fremy salt also converts the indoline back to the indole resulting in **6** as the final product. Aziridination of **6** to afford **3** was carried out with aziridine under aerobic conditions (reductive addition of aziridine followed by air oxidation to the quinone).

Hydrolytic Chemistry of Aziridinyl Quinones. The hydrolysis of the quinone forms of **1**−**4**, along with DZQ, were studied over the pH range of ∼0−7.4 in aerobic aqueous buffer at 30 °C with varying amounts of KCl added as the nucleophile. The goals were to determine pK_a values for the protonated aziridinyl quinones from pH−rate data and to determine the relationship between electronic character and the rate of nucleophile trapping. It has been assumed by others that the pK_a value for the protonated aziridinyl quinone is well below 0 (*32*). Our findings indicate that the protonated aziridinyl quinones possess pK_a values in the range of 0−5. This finding is consistent with the enhanced cross-linking of DNA by aziridinylbenzoquinones at pH values of ∼4 (*33*, *34*). Electrochemical studies previously provided protonated aziridinylbenzoquinone pK_a values in the range of 2.4−4.0 (*35*). The determination of pK_a values by kinetic means, as described below, offers an advantage over electrochemical methodology because the rapid hydrolysis of the aziridinylbenzoquinone in strong acid is not a limiting factor.

Aziridinyl quinone **1** afforded a mixture of the chloride-trapping (**1A**) and water-trapping (**1B**) products in aqueous buffer in the presence of varying concentrations of potassium chloride. The reaction followed a first-order rate law when the course of the reaction was followed at 288 nm. The observed first-order rate constants (k_{obsd}) were dependent on the concentration of chloride, and plots of k_{obsd} vs [chloride] provided the second rate constant for chloride trapping as the slope and the first-order rate constant for water trapping as the *y*-intercept. Shown in Figure 1 is a log plot of these observed first-order rate constants as a function of pH. The negative slopes of the chloride- and water-trapping plots indicate that product formation occurs from the protonated species as illustrated in Scheme 3.

As the concentration of the acid increases, the quinone becomes completely protonated resulting in the plateau evident in Figure 1. The rate law for this process is shown in eq 1

$$k_{obsd} = \frac{a_H(k_1[\text{chloride}] + k_2[H_2O])}{a_H + K_{a1}} \qquad (1)$$

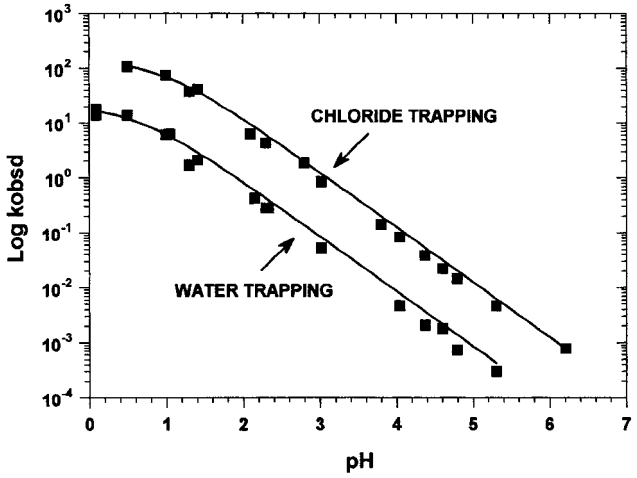

FIGURE 1: Log plots of the second-order rate constant for chloride trapping and of the pseudo-first-order rate constant for water trapping by **1** as a function of pH. Solid lines were computer-generated from eq 1.

Scheme 3

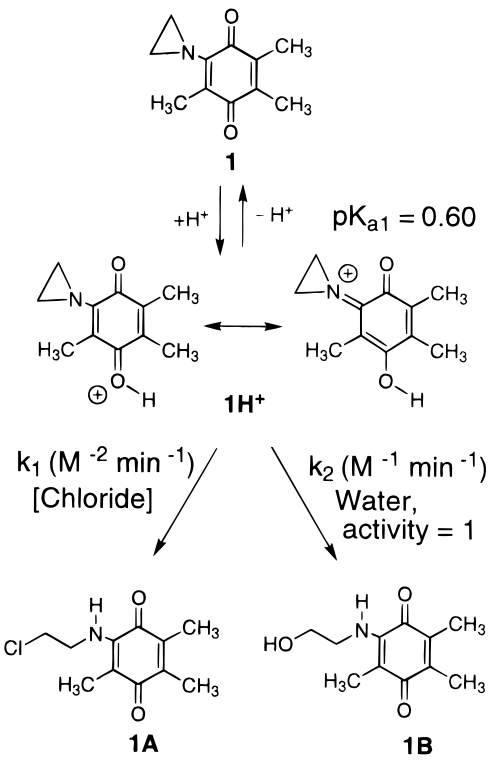

where k_1, k_2, and K_{a1} are constants found in Scheme 3 and a_H is the proton activity determined with a pH meter. Computer fitting of the data in Figure 1 to eq 1 provided k_1 = 151 M^{-2} min^{-1}, k_2 = 21.4 M^{-1} min^{-1}, and pK_{a1} = 0.60. These parameters were used to generate the solid curves shown in Figure 1 for chloride and water trapping of the protonated aziridinyl quinone.

The structure of the protonated aziridinyl quinone is considered to be an *O*-protonated species, the cation of which would be stabilized by delocalization. In contrast an *N*-protonated species, which is not capable of delocalization, was previously proposed for the protonated aziridinyl quinone (*32*, *36*, *37*). The results provided below are consistent with *O*-protonation because the pK_a is very sensitive to the quinone ring system structure (naphtho-

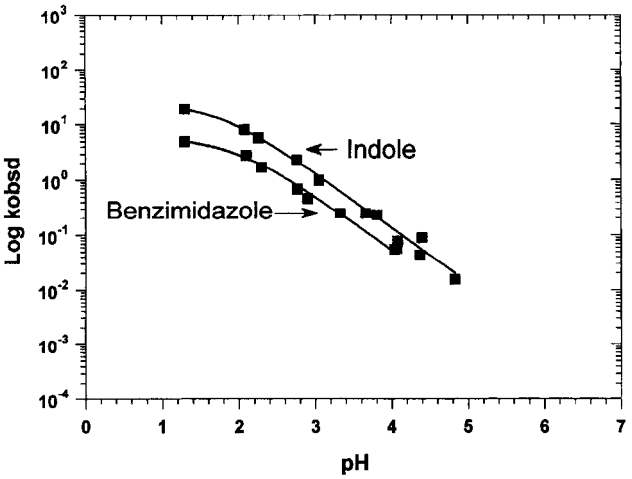

FIGURE 2: Log plots of the second-order rate constant for chloride trapping by the indole **3** and the benzimidazole **2** as a function of pH. Solid lines were computer-generated from eq 1 without the contribution of the water-trapping term.

quinone, benzoquinone, indoloquinone, benzimidazoquinone) and substituents, suggesting the presence of delocalization. In fact, another report postulated carbonyl oxygen protonation based on analogy to amides (*38*).

Reviewers comments on these kinetic studies are noteworthy. An alternative mechanism for the acid-catalyzed aziridinyl quinone ring opening was suggested involving both *N*- and *O*-protonation, with only the former actually undergoing the ring opening. This mechanism is kinetically indistinguishable from the process in Scheme 3 since both have a singly protonated transition state. *N*-Protonation, if it does occur, would be associated with a pK_a value much less than 0, and therefore the second-order rate constants for trapping of the protonated species at pH values > 5 would have to be at or near diffusion control. Other comments pertain to the influence of buffer species and ionic strength on aziridinyl quinone ring opening. The buffer species are held constant throughout an experiment, so rate changes only pertain to the variable concentration of chloride. The ionic strength does change as the chloride is varied, and the influences of ionic strength and chloride trapping on the rate are impossible to separate. However, at plateaus in the pH−rate profiles, where chloride trapping is constant, changes in ionic strength do not influence the rate of aziridine ring opening.

Shown in Figure 2 are pH−rate data for the benzimidazole (**2**) and indole (**3**) aziridinyl quinones. These data, along with those for the naphthoquinone (not shown), provided additional pK_a values and third-order rate constants for chloride trapping. We used these pK_a and chloride-trapping data to construct a free energy plot for chloride trapping by the protonated aziridinyl quinones. The cations resulting from carbonyl protonation of the indoloquinone, benzimidazoquinone, and naphthoquinone systems are stabilized by resonance and electron release by nitrogen lone pairs, Chart 3. The benzimidazole system was presumed to be protonated at the N3 position of the fused imidazo ring, since benzimidazole quinones are known to be *N*-protonated with a pK_a range of 0−2 for the resulting protonated species (*39*, *40*).

The pH−rate profiles for chloride trapping shown in Figure 2 followed the rate law in eq 1 (water-trapping rate constants k_2 were ignored). Computer fitting of the pH−rate data in Figure 2 to eq 1, considering only the contribution of the chloride-trapping term, provided the solid lines in this figure where $k_1 = 50$ M^{-2} min^{-1} and p$K_{a1} = 1.3$ for **2**; $k_1 = 20$ M^{-2} min^{-1} and p$K_{a1} = 1.9$ for **3**. The chloride trapping of the aziridinyl naphthoquinone **4** was also measured providing the following constants: $k_1 = 20$ M^{-2} min^{-1} and p$K_{a1} = 1.7$ (pH−rate profile not shown).

Chart 3

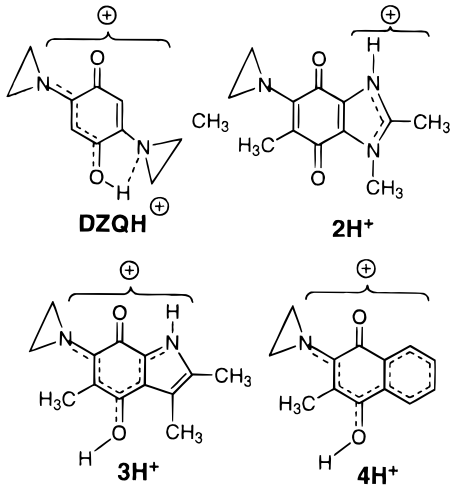

The DZQ trapping of chloride and water is a complex process involving the sequential opening of the aziridinyl rings as illustrated in Scheme 4. Previous kinetic studies of DZQ hydrolysis were carried out employing HPLC measurements (*41*), but the inflection due to the presence of an acid dissociation was not readily discernible from this study. The disappearance of DZQ was followed at 342 nm, and absorbance versus time (min) plots were fit to two consecutive rate laws. The first-order rate constants representing the first kinetic phase (k_{obsd}) were dependent on the concentration of chloride, and plots of k_{obsd} vs [chloride] provided the second-order rate constant for chloride trapping as the slope and the first-order rate constant for water trapping (activity of water = 1) as the *y*-intercept. Similarly the first-order rate constants representing the second kinetic phase provided the rate constants for opening of the second aziridine ring. Rate constants thus obtained were then plotted as the log versus pH to provided the four pH−rate profiles found in Figures 3 and 4.

The mechanism in Scheme 4 was used to derive the complete rate law for chloride and water opening of the first aziridine of DZQ, eq 2:

$$k_{obsd} = \frac{a_H K_{a2}(k_1[\text{chloride}] + k_2[H_2O]) + a_{H2}(k_3[\text{chloride}] + k_4[H_2O])}{a_{H2} + K_{a1}a_H + K_{a1}K_{a2}} \quad (2)$$

Inspection of the pH−rate data for the first phase in Figure 3 reveals the absence of any clear inflections in the chloride-trapping plot, which would indicate the presence of acid dissociation constants shown in eq 2. The solid line passing through the chloride data in Figure 3 was in fact generated from the linear relationship, $k_{obsd} = a_H(K)$, where K is a constant. However, close inspection of the chloride-trapping plot reveals that the data fall below the solid line at pH values > 4, suggesting that an inflection might be present. In fact,

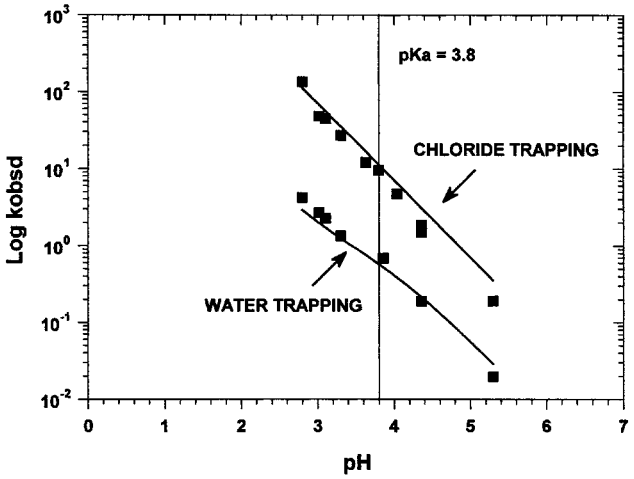

FIGURE 3: Log plots of the second-order rate constant for chloride trapping and of the pseudo-first-order rate constant for water trapping by the first aziridine ring of DZQ as a function of pH. The solid line for chloride trapping was computer-generated from a linear relationship, while that of water trapping was generated from eq 3.

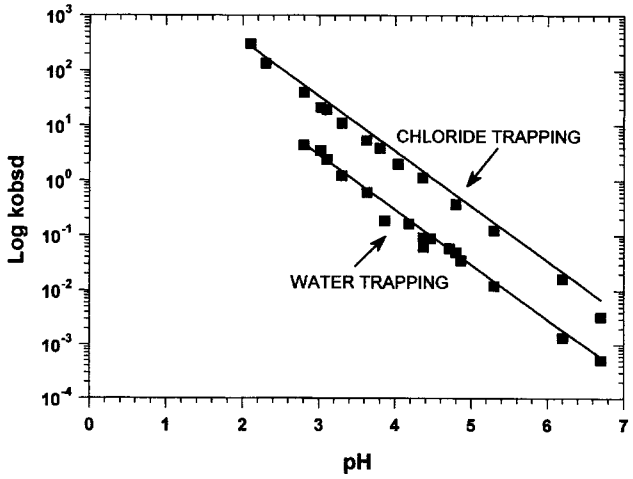

FIGURE 4: Log plots of the second-order rate constant for chloride trapping and of the pseudo-first-order rate constant for water trapping by the second aziridine ring of DZQ as a function of pH. The solid lines for chloride and water were both computer-generated from a linear relationship.

the water-trapping data in the same figure clearly shows the presence of such an inflection. Protonation of the second nitrogen of DZQ to afford $DZQH_2^{2+}$ results in chloride nucleophile-trapping rates which overwhelm the inflection due to the acid dissociation from $DZQH^+$ resulting in a pH−rate profile with a slope of ~ -1. Only in the case of the slower water-trapping rates is the inflection observed, followed by a slope of -1 in the pH−rate profile due to trapping of water by $DZQH_2^{2+}$. These data were fit to eq 3, which is an approximation of eq 2, where the first term pertains to water trapping of $DZQH^+$ and the second term pertains to water trapping by $DZQH_2^{2+}$ in which K is a collection of constants ($= k_4/K_{a2}$ when $a_H < K_{a2}$, i.e., the

Scheme 4

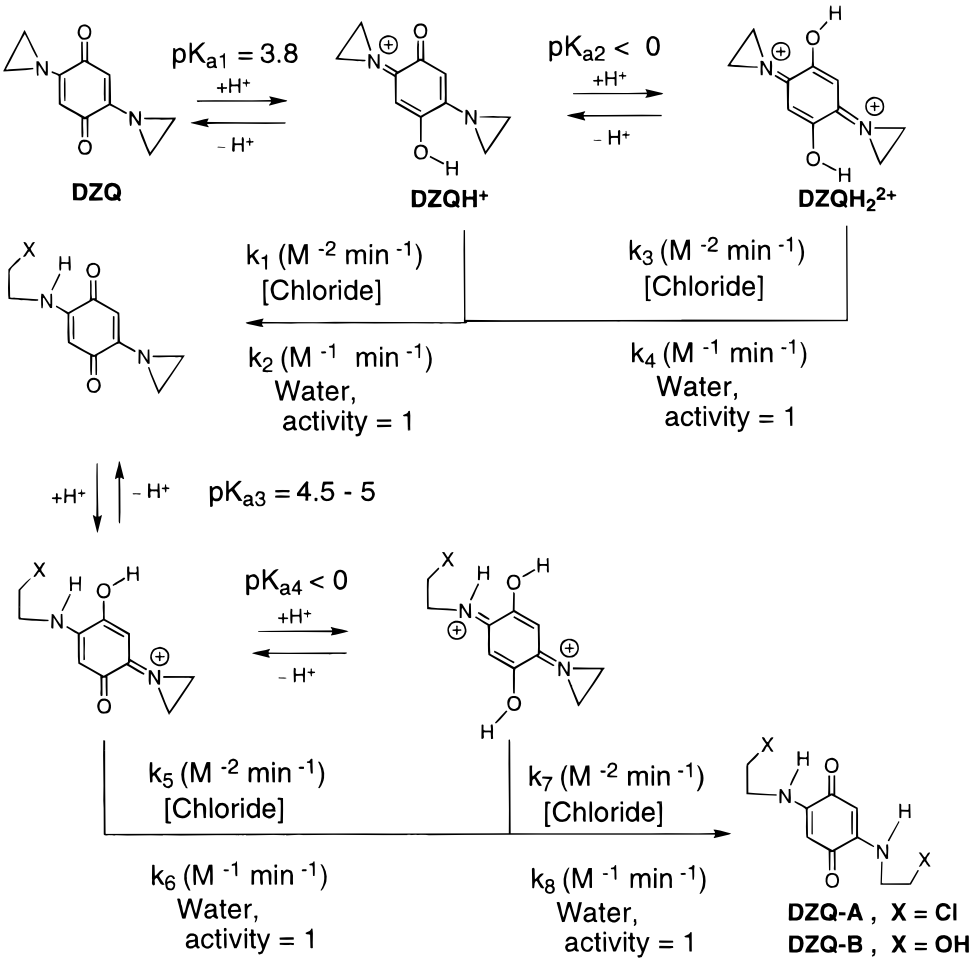

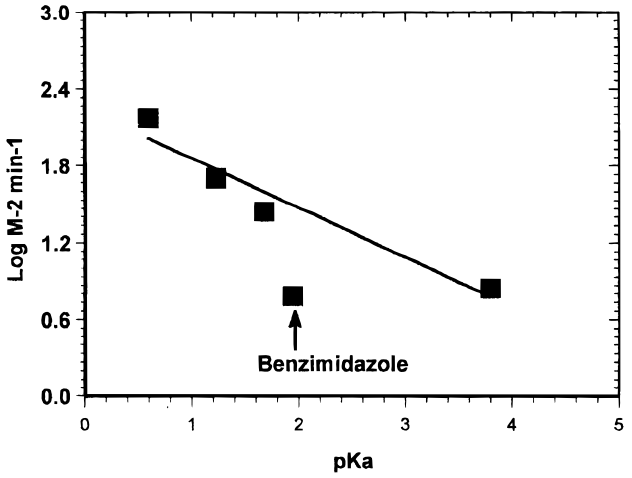

FIGURE 5: Linear free energy relationship between the ring opening of the protonated aziridinyl quinone by chloride (M^{-2} min^{-1}) versus pK_a. Aziridinyl quinones **1**, **3**, **4**, and DZQ follow the linear relationship, while the benzimidazole **2** deviates from the relationship.

acid activity is below the acid dissociation constant for $DZQH_2^{2+}$).

$$k_{obsd} = \frac{a_H k_2[H_2O]}{a_H + K_{a1}} + a_H K \qquad (3)$$

The solid line passing through the water-trapping data in Figure 3 was computer-generated from eq 3 where $k_2 = 0.70$ M^{-1} min^{-1}, p$K_{a1} = 3.8$, and $K = 1435$. Chloride trapping by $DZQH^+$ must also be associated with p$K_{a1} = 3.8$, and k_1 is estimated to be 7 M^{-2} min^{-1} based on the 10-fold difference between chloride and water trapping seen in the profiles in Figure 3. We expected that the relatively electron-rich DZQ would possess a higher pK_a than the aziridinyl quinones **1**−**4**, and therefore the value of p$K_{a1} = 3.8$ determined for the monoprotonated DZQ ($DZQH^+$) from this inflection seems reasonable. Indeed, the electron−rich quinone mitomycin C possesses an acid dissociation of 3.1 for the monoprotonated quinone (*42*).

pH−Rate data for the opening of the second aziridine ring of DZQ, the second kinetic phase of the consecutive two first-order processes, are provided in Figure 4. Both curves are essentially straight lines with a slope of −1. Opening of the first aziridine ring results in an electron-rich system since the amine lone pair is more available for delocalization than that of the aziridine nitrogen. Therefore the acid dissociation from the monoprotonated form, pK_{a3}, should be higher than 3.8. Between the pH values of 4 and 5 there is deviation of the data for chloride trapping from the curve suggesting the presence of an inflection, with k_5 (Scheme 4) approximately = 5 M^{-2} min^{-1}. This datum, 5 M^{-2} min^{-1} at p$K_{a3} = 4.5$, falls on the free energy plot discussed below.

The free energy plot in Figure 5 was obtained by plotting the log of the third-order rate constant for chloride trapping, k_1 (M^{-2} min^{-1}), versus pK_{a1} for the protonated quinone obtained from pH−rate data. The pK_{a1} values obtained from pH−rate data are considered to be actual values rather than collections of constants (*43*). Previous findings, consistent with a protonated aziridinyl quinone pK_a value in the range of 0−1, were obtained from electrochemical studies of a wide structural range of aziridinyl quinones (*32*). Two-electron reduction potential plots versus pH in fact show an inflection in this range (see p 262 of ref *32*). Mechanistically identical processes should fall on the same free energy plot. Thus, the benzoquinone **1**, the naphthoquinone **4**, the indoloquinone **3**, and DZQ all fall on this curve. As the pK_a of the protonated aziridinyl quinone decreases, the free energy of the protonated species increases and so does the rate constant for nucleophile trapping. The benzimidazoquinone **2** falls below the free energy plot because protonation of the fused imidazo ring, rather than the carbonyl oxygen, occurs. The resulting cation facilitates aziridine ring opening electrostatically rather than by through conjugation, and therefore the rate of aziridine ring opening is less than that predicted by the free energy plot. The benzimidazole aziridinyl quinone **2** also differs from the other quinones studied with respect to its ability to alkylate DNA in high yield, which we attribute to the protonated imidazo ring.

After an aziridinyl quinone traps a nucleophile, a slower hydrolysis reaction occurs resulting in replacement of the opened aziridine ring with a hydroxyl group on the benzoquinone system, Scheme 5. This hydrolysis reaction is crucial for the eventual synthesis of DNA bearing a cationic backbone substituent. All of the aziridinyl quinones studied undergo this reaction: adducts of DZQ and trimethylbenzoquinone **1** hydrolyze rapidly only in strong acid. For aziridinyl quinone adducts of **2** and **3**, the hydrolysis to **7** and **8**, respectively, is measurable over the pH range of 2−6. The pH−rate profiles for the hydrolysis of the benzimidazole adduct and the indole adduct are shown in Figure 6. Illustrated in Scheme 5 are the two hydrolysis mechanisms for these adducts: the carbonyl protonation and the benzimidazole protonation mechanisms. The indole adduct hydrolysis occurs by a simple acid-catalyzed process: equilibrium protonation of the quinone (p$K_a = 2.96$) followed by addition of water at 1.25 M^{-1} min^{-1} and then elimination of the amine leaving group. In contrast, the protonated benzimidazole is attacked by both water and hydroxide giving rise to the two plateaus observed in the pH−rate profile of Figure 6. The high pH plateau observed for benzimidazoquinone adduct hydrolysis is the reason that DNA bearing a cationic backbone substituent can be synthesized from such adducts under mild conditions.

Consideration of a hydrolysis mechanism involving equilibrium protonation of the benzimidazole followed by the attack by either water or hydroxide provides the rate law in eq 4:

$$k_{obsd} = \frac{a_H k_{H_2O}[H_2O] + a_H k_{HO}[K_w/a_H]}{a_H + K_{a1}} \qquad (4)$$

where pK_{a1} is the acid dissociation constant of the protonated benzimidazole, K_w is the autoprotolysis constant of water, a_H is the proton activity determined with a pH meter, and k_{H_2O} and k_{HO} are constants in Scheme 5. Computer fitting of the data in Figure 6 to eq 4 provided p$K_{a1} = 2.38$, k_{H_2O} = 0.04 M^{-1} min^{-1} (activity of water = 1), and $k_{HO} = 3.9 \times 10^9$ M^{-2} min^{-1}. This solution was used to generate the solid line in Figure 6. A problem with this mechanism is the near-diffusion-controlled rate required for the reaction of hydroxide with protonated benzimidazoquinone, both of which are present at very low concentrations at pH 4−5. Alternatively,

Scheme 5

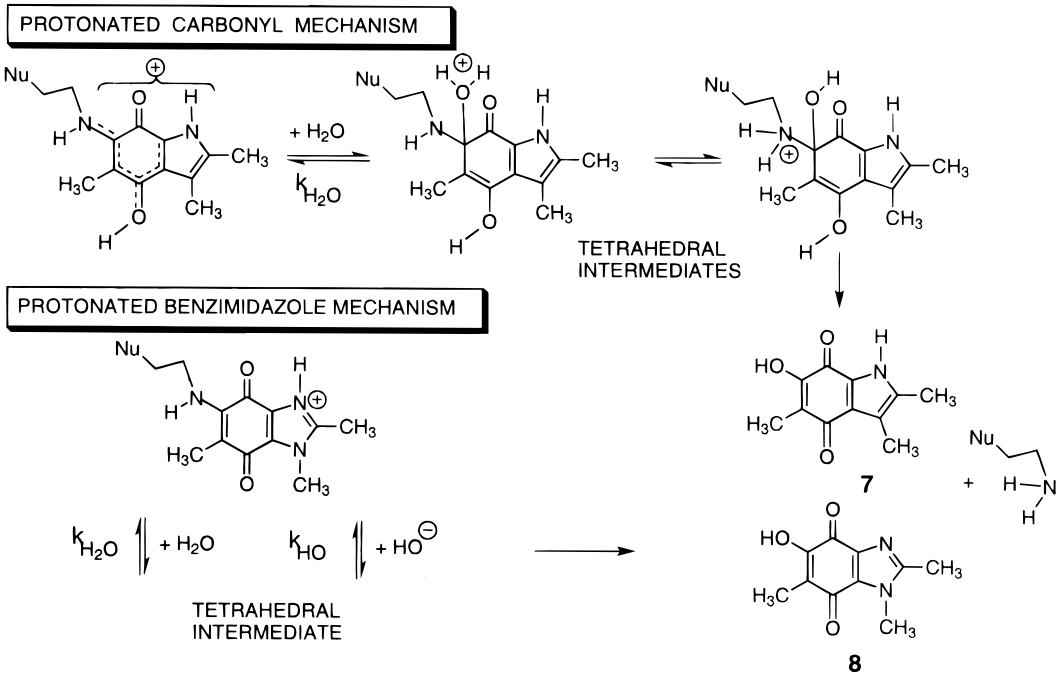

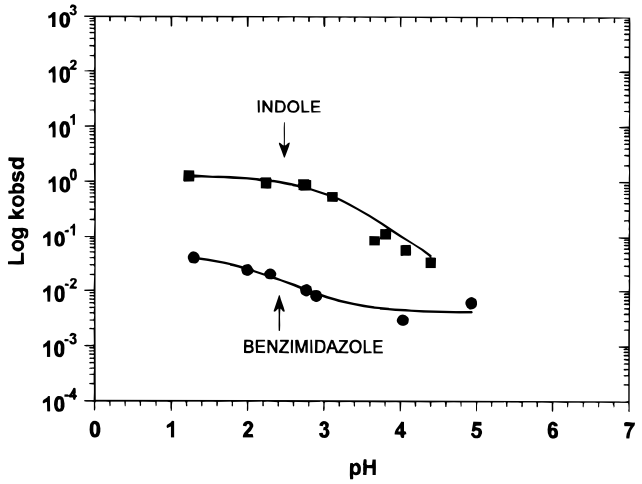

FIGURE 6: Log plots of the first-order rate constants for hydrolysis of the aziridine ring-opened forms of indole **3A** and benzimidazole **2A** as a function of pH. The solid line for the hydrolysis of **3A** was computer-generated from a single pK_a rate law with product formation occurring from the protonated species (analogous to eq 1), while that of **2A** was computer-generated from eq 4.

one may consider a water-catalyzed process where water acts as a general acid and protonates a quinone carbonyl while the addition of water is occurring.

Reaction of Aziridinyl Quinones with DNA Nucleophiles. Aziridinyl quinones, such as DZQ and related systems, have been known to alkylate DNA without reductive activation (*10*, *33*, *44*). Acidic conditions are required for DNA alkylation to occur (*33*), consistent with the pH−rate profiles presented above. There is evidence that multiple adducts form with AZQ; two major products and eight minor products were documented in one study (*44*). Only recently a DZQ−DNA cross-link involving N(7)- to N(7)-guanine linkages was characterized by mass spectrometry (*10*). In the present study, we looked at the ability of **1**−**4** and DZQ to alkylate poly(dG-C)·poly(dG-C) and poly(dA-T)·poly(dA-T) alternating polymers as well as a hexamer, with which NMR studies were carried out. The goals of these studies were to compare the DNA-alkylating capability and alkylation sites of these structurally diverse aziridinyl quinones.

The first study involved the reaction of **1** and DZQ with 5′-dGMP in order to test the influence of electronic character on nucleophile selectivity. Neither aziridinyl quinone provided high yields of nucleotide adducts with hydrolytic ring opening of the aziridine being the major feature. Quinone **1** is more electron-deficient than DZQ, based on the relative pK_a values of the protonated forms, resulting in different nucleophile selectivity. As illustrated in Scheme 6, DZQ reacts at the N(7)-position of 5′-dGMP to afford **9** upon adduct hydrolysis, while **1** traps phosphate and/or N(7) nucleophiles to afford **10**, **11**, and **12**.

The findings cited above do not necessarily indicate the DNA adducts formed with these aziridinyl quinones. The finding is consistent with previous findings reported by this laboratory, that electron-deficient alkylating agents react preferably at the phosphate backbone (*12*).

The next part of the study was to measure the amount of alkylation of poly(dG-C)·poly(dG-C) and poly(dA-T)·poly(dA-T) alternating polymers by each aziridinyl quinone. Treatment of each DNA with the aziridinyl quinones was carried out at 30 °C in 0.05 M pH 3.96 acetate buffer over a period time required for complete hydrolysis of the aziridinyl quinone (times obtained from pH−rate data). Thus the aziridinyl quinones either trap a DNA nucleophile or react with water during the incubation time. The alkylated DNAs are colored red or blue, permitting the determination of alkylation percentages from absorbance and extinction coefficient data, Table 1.

These alkylated DNAs are stable to mild hydrolysis (30 °C in water for 24 h) suggesting the presence of alkylated phosphates, which are more stable to hydrolysis than N(7)-adducts (*13*). In fact, the DZQ adducts are insoluble in aqueous solvents, consistent with neutralization of the anionic phosphate backbone. Inspection of the results in Table 1

Scheme 6

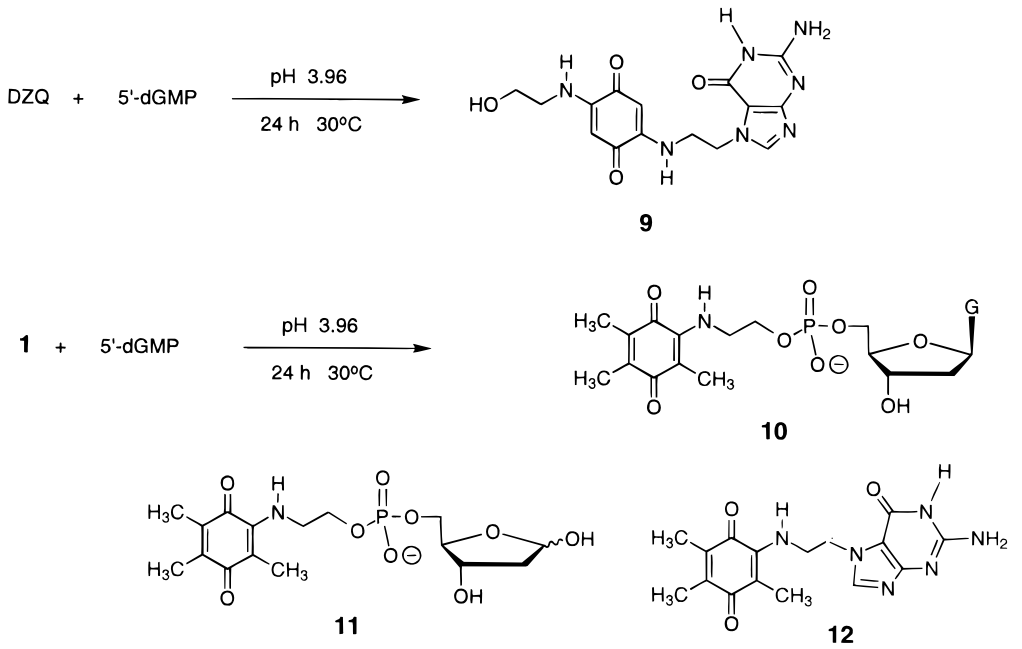

Table 1: Percentages of DNA Alkylation by Aziridinyl Quinones

aziridinyl quinone	% poly(dG-C)·poly(dG-C)	λ_{max} alkylated G-C	% poly(dA-T)·poly(dA-T)	λ_{max} alkylated A−T
1	17	600	6	600
2	22	570	35	570
3	0		0	
4	4	480	8	480
DZQ	20	503	16	487

reveals that the benzimidazoquinone (**2**) and DZQ are the best alkylating agents of both A-T and G-C base pairs. The indoloquinone **3** and the naphthoquinone **4**, on the other hand, do not alkylate DNA to a significant degree due to their insolubility in water. Although **1** is more soluble in water, this quinone does not alkylate DNA to the same degree as **2** and DZQ. These results are explained by the complexation of the protonated forms of **2** and DZQ in the major groove, bringing the aziridine group close to a phosphate oxygen. In fact, protonated reduced DZQ and related analogues are proposed to hydrogen bond in the major groove resulting in N(7) alkylation at specific base pairs (*5*). Shown in Figure 7 is the protonated form of **2** in the major groove of a GC base pair. This unminimized structure shows hydrogen bonding of protonated **2** to the cytosine amino group and the guanine carbonyl resulting in placement of the aziridine group close to the phosphate backbone. Generally, such docked structures are not minimized since in the absence of a covalent bond there are virtually no constraints on the possible molecular interactions (see p 41 of ref *45*).

Evidence of phosphate alkylation was obtained from $^{1}H-^{31}P$ correlation spectra. The presence of additional proton−phosphorus couplings at 3.7−3.9 ppm, the typical chemical shift range for the ethylene linkage resulting from aziridine ring opening, is taken as evidence of phosphotriester formation. No other proton chemical shifts of DNA, showing coupling to phosphorus, fall in this region. To prove phosphate alkylation by protonated aziridinyl quinones, excess DZQ was combined with $d(CGATCG)_2$ in 0.05 M

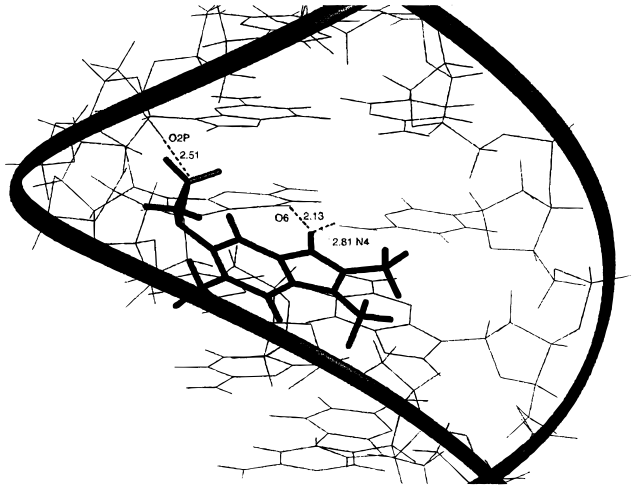

FIGURE 7: Unminimized structure of protonated **2** in the major groove of a GC base pair of $d(GGGCCC)_2$. The structure shows that the interaction of protonated **2** in the major groove will bring the aziridine close to the phosphate backbone.

pH 3.96 acetate buffer (see Materials and Methods). After a 12-h incubation, red-colored DNA was isolated from the reaction by precipitation/centrifugation. This DNA thus obtained was only partially soluble in small volumes (~0.7 mL) of water, and therefore the insoluble material was removed by centrifugation. A $^{1}H-^{31}P$ correlation spectrum, shown in plot B of Figure 8, obtained on the supernatant revealed the presence of one alkylated phosphate at 0.4 ppm (versus phosphoric acid) coupled to a methylene at δ 3.82. The dotted line in Figure 8 passes through this triplet, produced by coupling with the other methylene of the ethylene bridge. Comparison of plot B with the $^{1}H-^{31}P$ correlation spectrum of the native hexamer in plot A reveals the absence of a phosphorus chemical shift at 0.4 ppm as well as high-field protons ($\delta < 3.9$) coupled to phosphorus. The positive ^{31}P chemical shift is attributed to phosphotriester formation, and similar values have been reported by this group (*12*) and others (*46*). The phosphorus chemical shifts of DNA are slightly upfield relative to phosphoric acid, ^{31}P

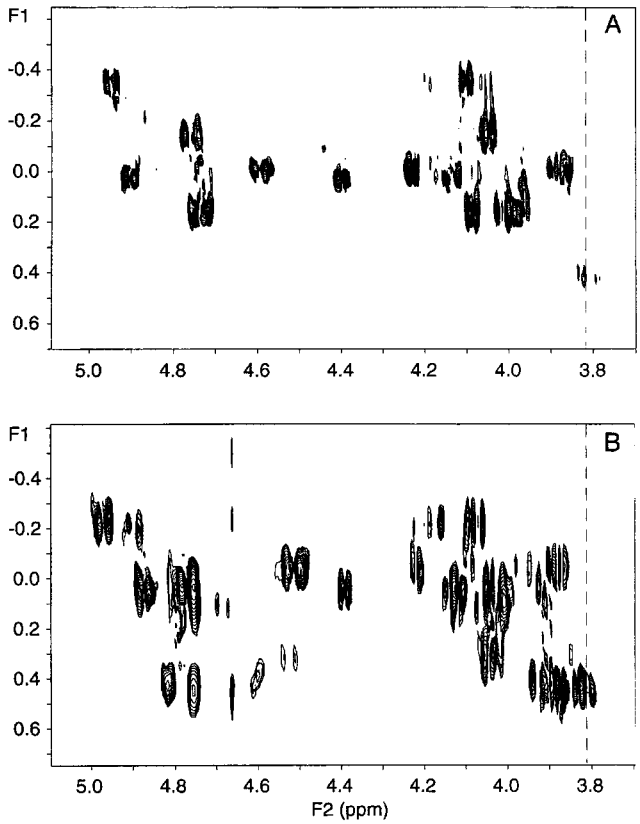

FIGURE 8: ^{1}H-Detected ^{1}H$-^{31}$P correlation spectra of native d(CGATGC)$_2$, plot A, and DZQ-treated d(CGATGC)$_2$, plot B, with $J = 20$ Hz. The dotted line passes through the methylene triplet of the ethylene tether. Note the presence of a trace impurity in the native DNA with protons at $\delta = 3.8$ coupled to phosphorus. This impurity is a phosphotriester resulting from incomplete ammonia deblocking of the synthetic DNA.

NMR reference at $\delta = 0.0$, while those of the phosphotriesters are downfield relative to this standard.

The findings enumerated above do not dismiss the importance of the guanine N(7) to N(7) cross-link determined previously for DZQ reactions with DNA (*10*) but suggest phosphate oxygen alkylation as an additional possibility. The model of DZQ bound to d(GGGCCC)$_2$ shown in Figure 9 suggests that initial guanine N(7) alkylation constrains the second aziridine of DZQ to the alkylation of another guanine N(7) center (see Figure 4 of ref *10*). Figure 9 also shows that the second aziridine is too far from the backbone for phosphate oxygen alkylation to occur. Isolation studies with DNA possessing this sequence resulted in the characterization of the N(7)- to N(7)-guanine DZQ cross-link (*10*). Initial phosphate alkylation, as shown in Figure 10, results in the second aziridine positioned too far (2.82 Å) from the nearest guanine N(7) center or from another phosphate oxygen for a second alkylation reaction. Therefore, barring any structural reorganization of the DNA, the second aziridine will merely react with water. Hydrolytic removal of DZQ−DNA adducts in strong acid and base, as previously employed (*10*), would hydrolyze this DZQ monoadduct from the phosphate backbone, and no evidence of these species would remain. In the present study, we employed hexamer without a run of G bases to avoid N(7) alkylation and did not subject the alkylated DNA to harsh conditions which would hydrolyze the phosphotriesters.

FIGURE 9: Minimized structure of alkylated d(GG**GC**C)$_2$ with DZQ attached at the guanine N(7) of the boldfaced GC base pair. The structure shows that the second aziridine can react with a second guanine N(7) but not with the phosphate backbone, which is too far away.

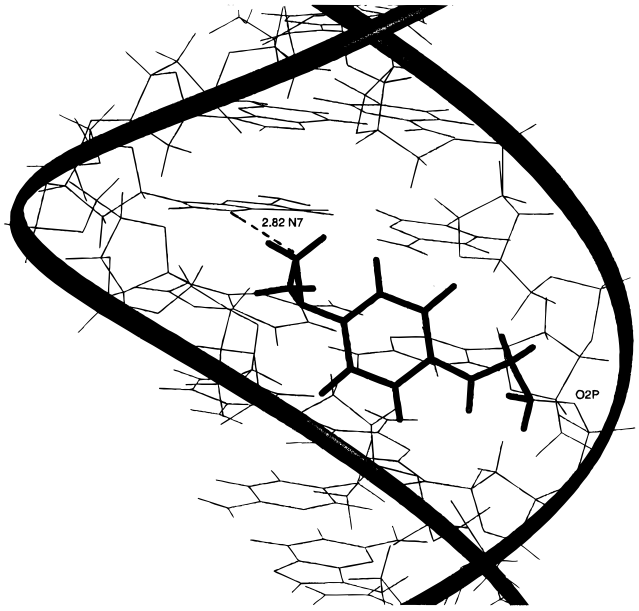

FIGURE 10: Minimized structure of alkylated d(GG**GC**C)$_2$ with DZQ attached at a phosphate oxygen of the boldfaced GC base pair. The structure shows that the second aziridine cannot quite reach a guanine N(7) unless reorganization of the DNA structure occurs.

Tagging the DNA Phosphate Backbone with the Aziridinylbenzimidazoquinone. In this section we discuss the conversion of DNA backbone phosphates to aminoethyl esters employing the aziridinylbenzimidazoquinone **2** as the reagent. In the previous section, we pointed out that protonated **2** can alkylate the DNA phosphate backbone in up to 35% yield. Hydrolytic studies described in another section revealed that the aziridine ring-opened product can be hydrolytically removed from the quinone moiety under mild conditions (see Figure 6). Taken together, these observations suggest that **2** could be employed as a reagent to tag the DNA backbone with aminoethyl phosphate esters. This possibility was initially explored with 5′-dGMP and GpC in order to determine NMR spectral changes associated with the tagging reaction. Finally, the tagging of the hexamer

Scheme 7

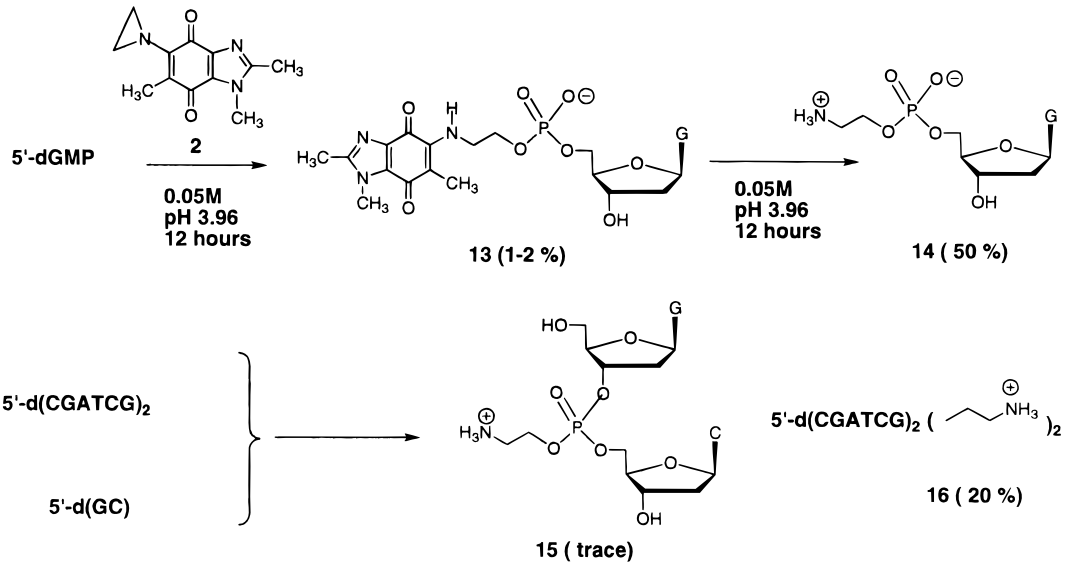

d(CGATCG)$_2$ was carried out to afford a 20% yield of aminoethyl phosphate esters. These studies are discussed below in conjunction with Scheme 7.

Alkylation of 5′-dGMP by **2** to afford the deep-blue nucleotide **13** proceeds in low yield (1−2%) due to the absence of a major groove for complexation of protonated **2** (see Figure 7) and the ongoing conversion of **13** to **14** during the reaction. A COSY NMR spectrum of purified **13** shows a "box" for the ethylene bridge, with coupling of the methylene next to the nitrogen (3.51 ppm, triplet) to the methylene attached to the phosphate oxygen (3.87 ppm, triplet). The latter resonance also shows coupling to phosphorus in the ^{1}H−^{31}P correlation spectrum. In whole DNA experiments, the ^{1}H−^{31}P correlation spectrum of the aziridinyl quinone alkylation product of **2** likewise shows phosphorus coupling to protons in the region of 3.8−3.9 ppm (see Figure 8). Purified **13** was converted to **14** by hydrolysis, and its purification was facilitated by the absence of 5′-dGMP, which had been removed in the purification of **13**. A COSY NMR spectrum of purified **14** also shows a "box" for the ethylene bridge, with coupling of the methylene next to the ammonium group (3.03 ppm, triplet) to the methylene attached to the phosphate oxygen (3.82 ppm, triplet). The alkylation of 5′-d(GC) by protonated **2** proceeded without giving any isolatable product because this 2-mer was present in small quantity. The ^{1}H NMR of recovered 5′-d(GC) did reveal the presence of the ethylene bridge: 3.02 ppm for the methylene bound to ammonium and 3.9 ppm for the methylene bound to phosphate oxygen. These studies assisted in the study of alkylation reactions of whole DNA by providing chemical shifts of the ethylene bridge. In the native DNA hexamer, the region from 3.0 to 3.5 ppm is free of proton resonances thereby permitting identification of the ethylene bridge.

Alkylation of the hexamer in Scheme 7 with protonated **2** afforded a deep-blue-colored product, which was characterized by ^{1}H NMR, ^{31}P NMR, ^{1}H−^{31}P correlation NMR, and UV−visible spectroscopy. The extinction coefficient for ring-opened **2** (**2A**, λ_{max} = 550 nm, ϵ = 1300) and absorbance data for the alkylated DNA indicated that there was a total of one alkylation per strand. This finding was supported by integration of the 1-methyl benzimidazole protons, which are clearly visible in the ^{1}H NMR spectrum of the alkylated hexamer. These results were used to determine that the alkylation yield per strand was 20%, since there are a total of five phosphates per strand. The ^{31}P NMR spectrum shows two new phosphorus resonances at 0.43 and 0.395 ppm (versus phosphate), typical values for DNA phosphotriesters (see Figure 8). Furthermore, these phosphorus centers are both coupled to ethylene bridge protons at 3.8 ppm. The formation of one adduct per six base pairs is not unreasonable considering that concomitant alteration of the DNA structure could restrict further alkylations.

In hydrolysis studies with relatively simple ring-opened forms of **2**, such as **13**, hydrolytic removal of the quinone ring was complete in about 12 h when incubated in pH 3.96 buffer at 30 °C. In contrast, **2**-alkylated DNAs were stable to hydrolysis under these conditions indefinitely. However, the blue hexamer discussed above was treated in 0 0.1 M pH 3.96 acetate buffer at 50 °C for 2 h resulting in complete removal of the quinone moiety. Apparently, the quinone ring is protected from hydrolytic attack in whole DNA, and heating along with denaturation is required to bring about hydrolysis. The DNA thus obtained was nearly colorless, and its ^{1}H NMR spectrum was missing the resonance associated with the 1-methyl group of the benzimidazole. However, the ^{31}P NMR still showed the triester phosphates, and the ethylene bridge was evident in a COSY experiment.

CONCLUSIONS

Hydrolytic studies of a series of aziridinyl quinones provides a compilation of the rate constants for nucleophile trapping and of the pK_a values for the protonated aziridinyl quinones. In most cases, carbonyl oxygen protonation occurs to afford a delocalized cation. An exception is the benzimidazoquinone derivative **2**, which was protonated at the fused imidazo ring instead of the carbonyl oxygen. Nucleophile-mediated opening of the aziridine ring therefore occurs by two mechanisms: nucleophile attack at the aziridine ring of the *O*-protonated quinone with electron flow from the nucleophile directly to the cationic center and nucleophile attack at the aziridine ring of the *N*-protonated quinone with

only an electrostatic interaction between the nucleophile and the cation. A linear free energy relationship obtained as a result of this study readily distinguishes between these mechanisms. The literature often shows aziridinyl quinone protonation occurring at the aziridinyl nitrogen (*33*, *37*, *41*), but the dependence of pK_a values on quinone substituents indicates the presence of delocalization, which must arise from *O*-protonation. Protonated DZQ has the relatively high pK_a value of 3.8, which is supported by both direct measurement and the linear free energy relationship. This pK_a value explains the enhanced cross-linking of DNA by DZQ and other aziridinyl quinones at pH 4 (*33*), at which nearly 50% of the aziridinyl quinone is in the protonated form.

Also investigated were the DNA alkylation reactions of protonated aziridinyl quinones. At the outset of this study, we postulated that these "hard" electrophiles would alkylate the phosphate backbone of DNA. Preliminary studies with the mononucleotide 5′-dGMP indicate that both the N(7) and phosphate oxygen are susceptible to alkylation in very low yield, with most of the aziridinyl quinone undergoing hydrolysis. Bulk DNA, on the other hand, is up to 35% alkylated as judged by the incorporation of the quinone chromophore into the DNA (see Table 1). These alkylated DNAs exhibit low solubility in aqueous buffer, and the chromophore is not readily released from the DNA, even after extended (days) incubation in aqueous buffers held at 30 °C. These properties are consistent with extensive phosphate alkylation, which was verified by a $^1H-^{31}P$ NMR correlation experiment with DZQ-alkylated hexamer. Our modeling studies present a new picture of DZQ alkylation of DNA, where there is competition between N(7) and phosphate alkylation. An N(7) alkylation event would restrict the second alkylation to the major groove perhaps (depending on the sequence) resulting in a second N(7) alkylation and cross-linking. In contrast, phosphate alkylation could be a dead end reaction because cross-linking is not likely unless there is structural reorganization of the DNA. Our contention is that DZQ phosphate adducts escape detection because the strong acid/base conditions employed in the workup of the alkylated DNA would destroy these adducts (*10*). The conclusions of this part of our study are that the phosphate backbone should be considered as a possible target of any DNA-alkylating agent and that an assessment of phosphate alkylation is best made with a $^1H-^{31}P$ NMR correlation experiment.

Our hydrolysis studies revealed that the benzimidazole-based aziridinyl quinone **2** undergoes a two consecutive first-order reaction: aziridine ring opening followed by hydrolytic removal of the aminoethyl group from the quinone ring. Since the latter reaction occurs under mild conditions, we considered using **2** as a reagent to tag the DNA phosphate backbone with aminoethyl groups. Such tags render anionic phosphates cationic and could also be employed as points of attachment for chromophores, spin labels, or other moieties to DNA. The main advantage of this reagent is the ease with which the tagging can be carried out (essentially a one-pot reaction). The last part of this study deals with the tagging of a hexamer and the spectroscopic characterization of the tags. The conclusion is that the tagging reagent works, but further work is needed to improve yields.

REFERENCES

1. Kim, H. S., and LeBreton, P. (1994) *Proc. Natl. Acad. Sci. U.S.A. 91*, 3725−3729.
2. Kim, H. S., Yu, M., Jaing, Q., and LeBreton, P. R. (1993) *J. Am. Chem. Soc. 115*, 6169−6183.
3. Broch, H., Hamza, A., and Vasilescu, D. (1996) *J. Biomol. Struct. Dyn. 13*, 903−914.
4. Hamza, A., Broch, H., and Vasilescu, D. (1996) *J. Biomol. Struct. Dyn. 13*, 915−924.
5. Hargreaves, R. H. J., Mayalarp, S. P., Butler, J., McAdam, S. R., O'Hare, C. C., and Hartley, J. A. (1997) *J. Med. Chem. 40*, 357−361.
6. Hartley, J. A., Berardini, M., Ponti, M., Gibson, N. W., Thompson, A. S., Thurston, A. S., Hoey, B. M., and Butler, J. (1991) *Biochemistry 30*, 11719−11724.
7. Lee, C.-S., Hartley, J. A., Berardini, M. D., Butler, J., Siegel, D., Ross, D., and Gibson, N. W. (1992) *Biochemistry 31*, 3019−3025.
8. Lee, C.-S., Pfeifer, G. P., and Gibson, N. W. (1994) *Cancer Res. 54*, 1622−1626.
9. Mayalarp, S. P., Hargreaves, R. H. J., Butler, J., O'Hare, C. C., and Hartley, J. A. (1996) *J. Med. Chem. 39*, 531−537.
10. Alley, S. C., Brameld, K. A., and Hopkins, P. B. (1994) *J. Am. Chem. Soc. 116*, 2734−2741.
11. Skibo, E. B. and Schulz, W. G. (1993) *J. Med. Chem. 36*, 3050−3055.
12. Schulz, W. G., Nieman, R. A., and Skibo, E. B. (1995) *Proc. Natl. Acad. Sci. U.S.A. 92*, 11854−11858.
13. Bannon, P., and Verly, W. (1972) *Eur. J. Biochem. 31*, 103−111.
14. Golding, B. T., Bleasdale, C., McGinnis, J., Muller, S., Rees, H. T., Rees, N. H., Farmer, P. B., and Watson, W. P. (1997) *Tetrahedron 53*, 4063−4082.
15. Swensen, D. H., and Lawley, P. D. (1978) *Biochem. J. 171*, 575−587.
16. Jensen, D. E., and Reed, D. J. (1978) *Biochemistry 17*, 5098−5107.
17. Hemminki, A., Vayrynen, T., and Hemminki, K. (1994) *Chem.−Biol. Interact. 93*, 51−58.
18. Barlow, T., and Dipple, A. (1998) *Chem. Res. Toxicol. 11*, 44−53.
19. Yates, J. M., Fennell, T. R., Turner, M. J., Recio, L., and Summer, S. C. J. (1994) *Carcinogenesis 15*, 277−283.
20. Uhlmann, E., Peyman, A., and Will, D. W. (1997) in *Encyclopedia of Cancer* (Bertino, J. R., Ed.) Vol. 1, pp 64−81, Academic Press Inc., San Diego, CA.
21. Rawls, R. L. (1997) *Chem. Eng. News* June 2, 35−39.
22. Nielsen, P. E. (1995) *Annu. Rev. Biophys. Biomol. Struct. 24*, 167−183.
23. Uhlmann, E., and Peyman, A. (1990) *Chem. Rev. 90*, 544−584.
24. Browne, K. A., Dempcy, R. O., and Bruice, T. C. (1995) *Proc. Natl. Acad. Sci. U.S.A. 92*, 7051−7055.
25. Fathi, R., Huang, Q., Coppola, G., Delaney, W., Teasdale, R., Krieg, A. M., and Cook, A. F. (1994) *Nucleic Acids Res. 22*, 5416−5424.
26. Freier, S. M., and Altmann, K. H. (1997) *Nucleic Acids Res. 25*, 4429−4443.
27. Wrigley, S. K., and ChicarelliRobinson, M. I. (1997) in *Annual Reports in Medicinal Chemistry* (Bristol, J. A., Ed.) Vol. 32, pp 285−294, Academic Press Inc., San Diego, CA.
28. Erion, M. D., Takabayashi, K., Smith, H. B., Kessi, J., Wagner, S., Honger, S., Shames, S. L., and Ealick, S. E. (1997) *Biochemistry 36*, 11725−11734.
29. Skibo, E. B., Islam, I., Heileman, M. J., and Schulz, W. G. (1994) *J. Med. Chem. 37*, 78−92.
30. Ockenden, D. W., and Schofield, K. (1953) *J. Chem. Soc.* 612−618.
31. Zimmer, H., Lankin, D. C., and Horgan, S. W. (1971) *Chem. Rev. 71*, 229−246.
32. Driebergen, R. J., Hartigh, J. D., Holthuis, J. J. M., Hulshoff, A., Van Oort, W. J., Postma Kelder, S. J., Verboom, W., Reinhoudt, D. N., Bos, M., and Van Der Linden, W. E. (1990) *Anal. Chim. Acta 233*, 251−268.

33. Akahtar, M. H., Begleiter, A., Johnson, D., Lown, J. W., McLaughlin, L., and Sim, S.-K. (1975) *Can. J. Chem. 53*, 2891−2905.
34. Lusthof, K. J., de Mol, N. J., Janssen, L. H. M., Verboom, W., and Reinhoudt, D. N. (1989) *Chem.−Biol. Interact. 70*, 249−262.
35. Driebergen, R. J. (1987) Qualitative and Quantitative Aspects of Structure−Electrochemistry−Cytotoxicity Relationships of Aziridinylquinones. Ph.D. Thesis, Utrecht.
36. Driebergen, R. J., Moret, E. E., Janssen, L. H. M., Blauw, J. S., Holthuis, J. J. M., Postma Kelder, S. J., Verboom, W., Reinhoudt, D. N., and Van Der Linden, W. E. (1992) *Anal. Chim. Acta 257*, 257−273.
37. Driebergen, R. J., Holthuis, J. J. M., Blauw, J. S., Verboom, W., and Van Der Linden, W. E. (1990) *Anal. Chim. Acta 234*, 285−307.
38. Rademacher, P., and Obe, G. (1995) *Mutat. Res. 340*, 37−49.
39. Lemus, R. L., Lee, C.-H., and Skibo, E. B. (1989) *J. Org. Chem. 54*, 3611−3618.
40. Lee, C. H., Gilchrist, J. H., and Skibo, E. B. (1986) *J. Org. Chem. 51*, 4784−4792.
41. Kusai, A., Tanaka, S., and Ueda, S. (1981) *Chem. Pharm. Bull. 29*, 3671−3679.
42. Boruah, R. C., and Skibo, E. B. (1995) *J. Org. Chem. 60*, 2232−2243.
43. Bruice, T. C., and Schimir, G. L. (1959) *J. Am. Chem. Soc. 81*, 4552−4556.
44. Gupta, R. C., Garg, A., Earley, K., Agarwal, S. C., Lambert, G. R., and Nesnow, S. (1991) *Cancer Res. 51*, 5198−5204.
45. O'Donnell, T. J. (1989) in *Computer-Aided Drug Design. Methods and Applications* (Perun, T. J., and Propst, C. L., Eds.) pp 19−54, Marcel Dekker, Inc., New York.
46. Jones, R. A. Y., and Katritzky, A. R. (1962) *Angew. Chem. 74*, 60−68.

BI981204J